

# Gd<sub>5</sub>Ni<sub>0.96</sub>Sb<sub>2.04</sub> and Gd<sub>5</sub>Ni<sub>0.71</sub>Bi<sub>2.29</sub>: Crystal structure, magnetic properties and magnetocaloric effect. Structural transformation and magnetic properties of hexagonal Gd<sub>5</sub>Bi<sub>3</sub>

Volodymyr Svitlyk, Fan Fei, Yuriy Mozharivskij\*

Department of Chemistry, McMaster University, ABB 423, 1280 Main Street west, Hamilton, Ontario, Canada, L8S 4M1

Received 12 November 2007; received in revised form 7 February 2008; accepted 10 February 2008

Available online 20 February 2008

## Abstract

Nickel was successfully introduced into the Gd<sub>5</sub>Sb<sub>3</sub> and Gd<sub>5</sub>Bi<sub>3</sub> binaries to yield the Gd<sub>5</sub>Ni<sub>0.96(1)</sub>Sb<sub>2.04(1)</sub> and Gd<sub>5</sub>Ni<sub>0.71(1)</sub>Bi<sub>2.29(1)</sub> phases. Both Ni-substituted compounds adopt the orthorhombic Yb<sub>5</sub>Sb<sub>3</sub>-type structure. While the Gd<sub>5</sub>Ni<sub>0.71</sub>Bi<sub>2.29</sub> phase is thermodynamically stable at 800 °C and decomposes at lower temperatures upon annealing, it can be easily quenched to room temperature by rapid cooling from 800 °C. The Gd<sub>5</sub>Ni<sub>0.96</sub>Sb<sub>2.04</sub> phase is found to be thermodynamically stable till room temperature. Through annealing at different temperatures, Gd<sub>5</sub>Bi<sub>3</sub> was proven to undergo the Mn<sub>5</sub>Si<sub>3</sub>-type (LT) ↔ Yb<sub>5</sub>Sb<sub>3</sub>-type (HT) transformation reversibly, whereas Gd<sub>5</sub>Sb<sub>3</sub> was found to adopt only the hexagonal Mn<sub>5</sub>Si<sub>3</sub>-type structure. Orthorhombic Gd<sub>5</sub>Ni<sub>0.96</sub>Sb<sub>2.04</sub> and Gd<sub>5</sub>Ni<sub>0.71</sub>Bi<sub>2.29</sub> and low-temperature hexagonal Gd<sub>5</sub>Bi<sub>3</sub> order ferromagnetically at 115, 162 and 112 K, respectively. In Gd<sub>5</sub>Bi<sub>3</sub>, the ferromagnetic ordering is followed by spin reorientation below 64 K. Magnetocaloric effect in terms of Δ*S* was evaluated from the magnetization data and found to reach the maximum values of −7.7 J/kgK for Gd<sub>5</sub>Ni<sub>0.96</sub>Sb<sub>2.04</sub> and −5.6 J/kgK for Gd<sub>5</sub>Ni<sub>0.71</sub>Bi<sub>2.29</sub> around their Curie temperatures.

© 2008 Elsevier Inc. All rights reserved.

**Keywords:** Gadolinium bismuthide; Gadolinium nickel antimonide; Gadolinium nickel bismuthide; Phase transitions; Structure; Magnetic properties; Magnetocaloric effect

## 1. Introduction

Discovery of the giant magnetocaloric effect in Gd<sub>5</sub>Si<sub>2</sub>Ge<sub>2</sub> and related phases [1,2] showed that cooling efficiency of a ferromagnetic material increases significantly if a ferromagnetic ordering is coupled to a first-order structural transition. For such materials, the total entropy change, Δ*S*, can be divided in two parts: Δ*S*<sub>mag</sub> and Δ*S*<sub>str</sub> associated with the magnetic and structural transitions, respectively. While it is difficult to introduce and control structural transformations and associated with them Δ*S*<sub>str</sub> in inorganic solid-state materials, it is possible to optimize the magnetic entropy part, Δ*S*<sub>mag</sub>. In general, large Δ*S*<sub>mag</sub> is associated with metal-rich phases, consisting of magnetically active 3*d*- or 4*f*- elements. Besides, the 4*f*-elements

are likely to yield a larger Δ*S*<sub>mag</sub> as the maximum entropy change during the ferromagnetic ordering depends on the total quantum number through Δ*S*<sub>mag</sub> = *R* ln(2*J* + 1) [3]. Driven by this argument, we initiated exploration of structural and magnetic properties of the Ni-substituted Gd<sub>5</sub>Sb<sub>3</sub> and Gd<sub>5</sub>Bi<sub>3</sub> phases. The study was also inspired, in part, by the fact that the structurally related Y<sub>5</sub>Sb<sub>3</sub> phase and its derivative Y<sub>5</sub>Ni<sub>*x*</sub>Sb<sub>3−*x*</sub> were found to undergo a first-order orthorhombic-to-hexagonal structural transition at elevated temperatures [4].

Similar to Y<sub>5</sub>Sb<sub>3</sub>, Gd<sub>5</sub>Bi<sub>3</sub> was found to adopt two structural modifications [5]. The stoichiometric Gd<sub>5</sub>Bi<sub>3</sub> phase was believed to adopt a hexagonal Mn<sub>5</sub>Si<sub>3</sub>-type structure, while a Gd-richer phase, Gd<sub>5+*x*</sub>Bi<sub>3</sub>, was suggested for the orthorhombic Yb<sub>5</sub>Sb<sub>3</sub>-type polymorph [5]. No other literature data were found to substantiate existence of Gd<sub>5+*x*</sub>Bi<sub>3</sub>, instead recent results by Szade and Drzyzga [6] indicated that a Yb<sub>5</sub>Sb<sub>3</sub>-type structure is

\*Corresponding author. Fax: +1 905 521 2773.

E-mail address: [mozhar@mcmaster.ca](mailto:mozhar@mcmaster.ca) (Y. Mozharivskij).

adopted by stoichiometric  $\text{Gd}_5\text{Bi}_3$  at higher temperatures. This high-temperature modification was found to exhibit a ferromagnetic-like transition at 110 K, followed by spin reorientation or freezing below 60 K [6]. The magnetic behavior of the low-temperature hexagonal  $\text{Gd}_5\text{Bi}_3$  polymorph was not studied. In contrast to  $\text{Gd}_5\text{Bi}_3$ , only a hexagonal  $\text{Mn}_5\text{Si}_3$ -type phase has been reported for  $\text{Gd}_5\text{Sb}_3$  [7]. This hexagonal  $\text{Gd}_5\text{Sb}_3$  phase orders ferromagnetically at 187 K and then undergoes a possible ferrimagnetic transition below 50 K [8]. Presence of structural and/or magnetic transitions in  $\text{Gd}_5\text{Sb}_3$  and  $\text{Gd}_5\text{Bi}_3$  was another motivation for us to explore the properties of the Ni-substituted phases. Here we report on the structural features and magnetocaloric effect of these phases.

## 2. Experimental

### 2.1. Synthesis and X-ray structure analysis

The starting materials were Gd (99.9%, CERAC Incorporation), Ni (99.93% Alfa Aesar), Bi (99.9999%, CERAC Incorporation) and antimony (99.999%, CERAC Incorporation). The samples with initial compositions  $\text{Gd}_5\text{Sb}_3$ ,  $\text{Gd}_5\text{Bi}_3$ ,  $\text{Gd}_5\text{NiSb}_2$  and  $\text{Gd}_5\text{NiBi}_2$  and a total mass of 1 g were arc melted in argon atmosphere, then turned over and remelted to achieve homogeneity. Two milligrams of Sb or Bi was added extra to the samples to compensate for losses during melting. For annealing at 800 °C and lower temperatures, the samples were sealed in evacuated silica tubes, kept at the required temperature for 1 or 2 weeks and then quenched in cold water. For annealing at 1350 °C, the samples were sealed in tantalum tubes with argon inside and heated in dynamic vacuum ( $10^{-6}$  Torr) in an induction furnace.

Phase composition and lattice constants of the prepared samples (Table 1) were determined from the X-ray powder diffraction patterns recorded on a Huber image plate Guinier camera with the  $\text{CuK}\alpha_1$  radiation. The lattice constants were derived through a full-profile Rietveld analysis using the Rietica software [9]. Single crystal studies were performed on a STOE IPDS II diffractometer with the  $\text{MoK}\alpha$  radiation. Small crystals with a shape of rectangular plates and silver luster were picked up from the  $\text{Gd}_5\text{NiSb}_2$  and  $\text{Gd}_5\text{NiBi}_2$  samples annealed at 800 °C for 2 weeks. The diffraction data were collected in the whole

reciprocal sphere. Using the SHELXL program [10], the compositions were refined to  $\text{Gd}_5\text{Ni}_{0.96(1)}\text{Sb}_{2.04(1)}$  and  $\text{Gd}_5\text{Ni}_{0.71(1)}\text{Bi}_{2.29(1)}$  for the  $\text{Gd}_5\text{NiSb}_2$  and  $\text{Gd}_5\text{NiBi}_2$  samples, respectively (Tables 2 and 3). While during the refinements Ni was found to occupy the 4c site, we also check for the Ni presence on the 8d Sb1 or Bi1 site by refining their occupancies (Ni presence would lead to a lower electron density and thus lower occupancies for the pure Sb1/Bi sites). The refined occupancies were 0.993(3) for the 8d Sb1 site in  $\text{Gd}_5\text{Ni}_{0.96(1)}\text{Sb}_{2.04(1)}$  and 0.995(6) for the 8d Bi1 site  $\text{Gd}_5\text{Ni}_{0.71(1)}\text{Bi}_{2.29(1)}$ . The occupancies are close to one within three standard deviations and thus the

Table 2

Crystal data and structure refinements for  $\text{Gd}_5\text{Ni}_{0.96(1)}\text{Sb}_{2.04(1)}$  and  $\text{Gd}_5\text{Ni}_{0.71(1)}\text{Bi}_{2.29(1)}$  at 293 K,  $\text{MoK}\alpha_1$  radiation, STOE IPDS II diffractometer

Composition	$\text{Gd}_5\text{Ni}_{0.96(1)}\text{Sb}_{2.04(1)}$	$\text{Gd}_5\text{Ni}_{0.71(1)}\text{Bi}_{2.29(1)}$
Space group	<i>Pnma</i>	<i>Pnma</i>
Lattice parameters (Å)	<i>a</i> = 12.136(1)	<i>a</i> = 12.228(2)
	<i>b</i> = 8.9472(7)	<i>b</i> = 9.241(1)
	<i>c</i> = 7.9546(7)	<i>c</i> = 8.137(1)
Volume (Å <sup>3</sup> )	863.7(3)	919.5(3)
Z	4	4
Density (calculated) (g/cm <sup>3</sup> )	8.389	9.665
Crystal size (mm <sup>3</sup> )	0.017 × 0.054 × 0.079	0.009 × 0.046 × 0.065
2θ range for data collection	6.12–58.22°	6.02–58.28°
Index ranges	−16 ≤ <i>h</i> ≤ 16, −12 ≤ <i>k</i> ≤ 11, −10 ≤ <i>l</i> ≤ 10	−16 ≤ <i>h</i> ≤ 16, −12 ≤ <i>k</i> ≤ 12, −11 ≤ <i>l</i> ≤ 11
Reflections collected	8646	8896
Independent reflections	1227 [ <i>R</i> <sub>int</sub> = 0.0603]	1306 [ <i>R</i> <sub>int</sub> = 0.2325]
Completeness to max 2θ (%)	99.5	99.5
Data/restraints/parameters	1227/0/45	1306/0/45
Goodness-of-fit on <i>F</i> <sup>2</sup>	0.812	0.699
Final <i>R</i> indices [ <i>I</i> > 2σ( <i>I</i> )]	<i>R</i> <sub>1</sub> = 0.0286, <i>wR</i> <sub>2</sub> = 0.0335	<i>R</i> <sub>1</sub> = 0.0479, <i>wR</i> <sub>2</sub> = 0.0547
<i>R</i> indices (all data)	<i>R</i> <sub>1</sub> = 0.0375, <i>wR</i> <sub>2</sub> = 0.0522	<i>R</i> <sub>1</sub> = 0.0727, <i>wR</i> <sub>2</sub> = 0.1345
Extinction coefficient	0.00054(3)	0.00013(2)
Largest diff. peak/hole, (e/Å <sup>3</sup> )	1.60/−2.18	2.93/−4.30

Table 1

Crystal data for the phases annealed at 800 and 1350 °C

Phase	Annealing temperature (°C)	Structure type	Space group	Lattice constants, Å
$\text{Gd}_5\text{Sb}_3$	800	$\text{Mn}_5\text{Si}_3$	<i>P6</i> <sub>3</sub> / <i>mcm</i>	<i>a</i> = 9.0243(1), <i>c</i> = 6.3241(1)
$\text{Gd}_5\text{Ni}_{0.96}\text{Sb}_{2.04}$	800	$\text{Yb}_5\text{Sb}_3$	<i>Pnma</i>	<i>a</i> = 12.133(1), <i>b</i> = 8.9528(8), <i>c</i> = 7.9561(8)
$\text{Gd}_5\text{Bi}_3$	800	$\text{Mn}_5\text{Si}_3$	<i>P6</i> <sub>3</sub> / <i>mcm</i>	<i>a</i> = 9.1842(7), <i>c</i> = 6.4177(8)
$\text{Gd}_5\text{Bi}_3$	1350	$\text{Yb}_5\text{Sb}_3$	<i>Pnma</i>	<i>a</i> = 12.106(1), <i>b</i> = 9.549(1), <i>c</i> = 8.261(1)
$\text{Gd}_5\text{Ni}_{0.71}\text{Bi}_{2.29}$	800	$\text{Yb}_5\text{Sb}_3$	<i>Pnma</i>	<i>a</i> = 12.230(1), <i>b</i> = 9.222(1), <i>c</i> = 8.102(1)

Table 3

Atomic and isotropic temperature ( $U$ ) parameters for  $Gd_5Ni_{0.96(1)}Sb_{2.04(1)}$  and  $Gd_5Ni_{0.71(1)}Bi_{2.29(1)}$  from single crystal diffraction data

Atom	Occupancy	$x/a$	$y/b$	$z/c$	$U$ ( $\text{\AA}^2$ )	
<i>Gd<sub>5</sub>Ni<sub>0.96(1)</sub>Sb<sub>2.04(1)</sub></i>						
Gd1	4c	1	0.2907(1)	1/4	0.6576(1)	0.010(1)
Gd2	4c	1	0.1991(1)	1/4	0.1299(1)	0.010(1)
Gd3	4c	1	0.5005(1)	1/4	0.9609(1)	0.010(1)
Gd4	8d	1	0.4338(1)	0.0390(1)	0.3156(1)	0.011(1)
Sb1	8d	1	0.3269(1)	0.9926(1)	0.9277(1)	0.009(1)
Sb2/Ni	4c	0.04/0.96(1)	0.5148(1)	1/4	0.5775(2)	0.012(1)
<i>Gd<sub>5</sub>Ni<sub>0.71(1)</sub>Bi<sub>2.29(1)</sub></i>						
Gd1	4c	1	0.2880(2)	1/4	0.6622(2)	0.019(1)
Gd2	4c	1	0.2025(2)	1/4	0.1331(3)	0.021(1)
Gd3	4c	1	0.4986(2)	1/4	0.9646(2)	0.016(1)
Gd4	8d	1	0.4352(1)	0.0446(2)	0.3165(2)	0.025(1)
Bi1	8d	1	0.3264(1)	0.9906(1)	0.9274(1)	0.014(1)
Bi2/Ni	4c	0.29/0.71(1)	0.0215(2)	1/4	0.9119(3)	0.015(1)

corresponding 8d site can be assumed to be fully occupied by Sb or Bi.

Further details of the crystal structure investigations can be obtained from the Fachinformationszentrum Karlsruhe, 76344 Eggenstein-Leopoldshafen, Germany, (fax: +49 7247 808 666; e-mail: [crysdata@fiz.karlsruhe.de](mailto:crysdata@fiz.karlsruhe.de)) on quoting the depository CSD number 418769 for  $Gd_5Ni_{0.96(1)}Sb_{2.04(1)}$  and 418770 for  $Gd_5Ni_{0.71(1)}Bi_{2.29(1)}$  and also from the supporting information.

## 2.2. Magnetic measurements

Magnetization for the field cooled (FC) polycrystalline pieces of hexagonal  $Gd_5Bi_3$ , orthorhombic  $Gd_5Ni_{0.96}Sb_{2.04}$  and  $Gd_5Ni_{0.71}Bi_{2.29}$  phases (all annealed at 800 °C) was measured at 100 Oe field between 2 and 320 K (350 K for  $Gd_5Ni_{0.96}Sb_{2.04}$  compound) on a Quantum Design SQUID magnetometer (Fig. 1). The transition temperatures were derived from the  $\partial M/\partial T$  vs.  $T$  plots and correspond to the maxima in these plots. To explore the nature of the magnetic ordering in hexagonal  $Gd_5Bi_3$ , magnetization curves were measured at 4.2 and 100 K in increasing and decreasing magnetic fields (Fig. 2).

Magnetocaloric effect for  $Gd_5Ni_{0.96}Sb_{2.04}$  and  $Gd_5Ni_{0.71}Bi_{2.29}$  was evaluated from the magnetization data. For this purpose, a series of magnetization versus magnetic field ( $M$  vs.  $H$ ) measurements was done around the ordering temperature with 5 K increments (Fig. 3). The magnetic field changed from 0 to 50,000 Oe with a 1000 and 2000 Oe step for  $Gd_5Ni_{0.96}Sb_{2.04}$  and  $Gd_5Ni_{0.71}Bi_{2.29}$ , respectively.

## 3. Results and discussion

### 3.1. Thermal stability and structures of $Gd_5Sb_3$ , $Gd_5Bi_3$ , $Gd_5Ni_{0.96}Sb_{2.04}$ and $Gd_5Ni_{0.71}Bi_{2.29}$

Temperature stability of  $Gd_5Sb_3$ ,  $Gd_5Bi_3$ ,  $Gd_5Ni_{0.96}Sb_{2.04}$  and  $Gd_5Ni_{0.71}Bi_{2.29}$  is summarized in Fig. 4 (see

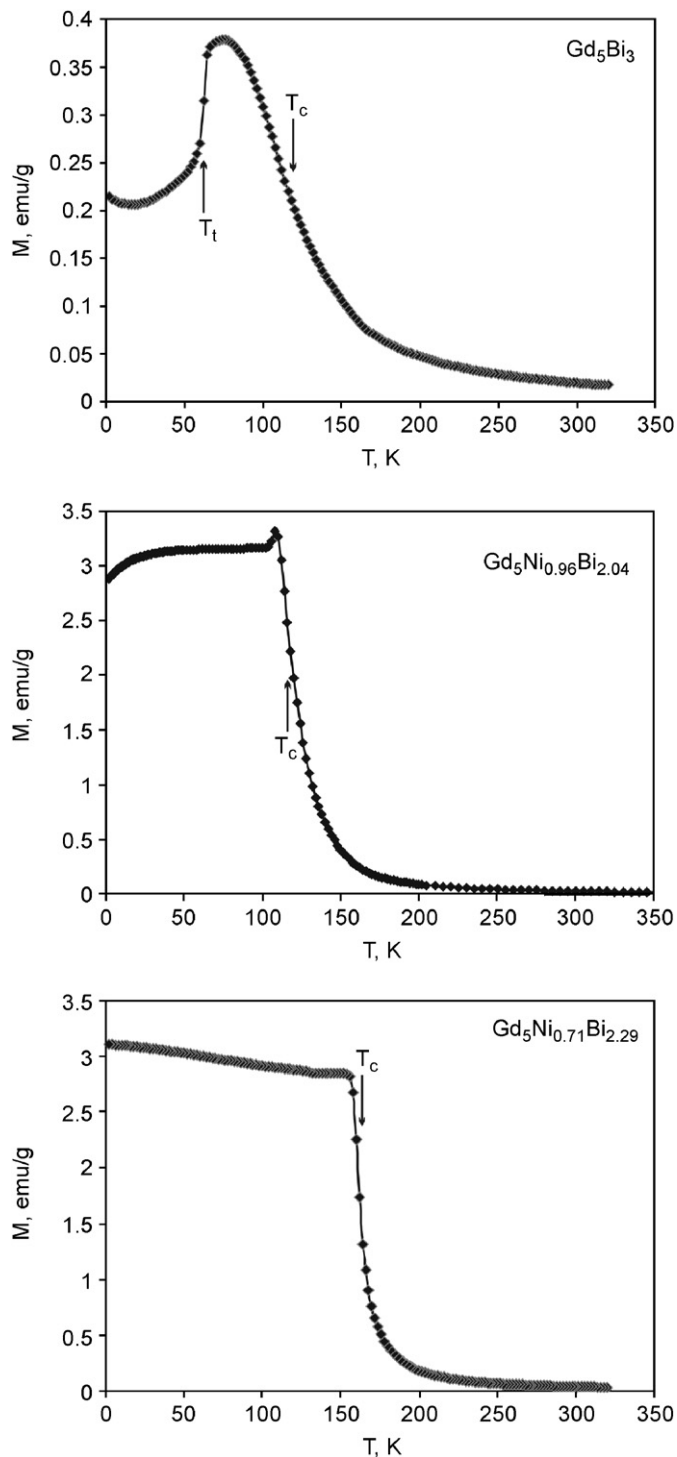


Fig. 1. Magnetization as a function of temperature at  $H = 100$  Oe for hexagonal  $Gd_5Bi_3$  and orthorhombic  $Gd_5Ni_{0.96}Sb_{2.04}$  and  $Gd_5Ni_{0.71}Bi_{2.29}$ .

also Table 1). From the initial annealing at 800 °C, both  $Gd_5Sb_3$  and  $Gd_5Bi_3$  were found to adopt the hexagonal  $Mn_5Si_3$ -type structure at 800 °C, while  $Gd_5Ni_{0.96}Sb_{2.04}$  and  $Gd_5Ni_{0.71}Bi_{2.29}$  were found to crystallize in the orthorhombic  $Yb_5Sb_3$ -type structure at 800 °C. Since hexagonal  $Mn_5Si_3$ -type and orthorhombic  $Yb_5Sb_3$ -type structures have been identified as low-temperature (LT) and high-temperature (HT) forms, respectively, for  $Y_5Sb_3$  [4], the

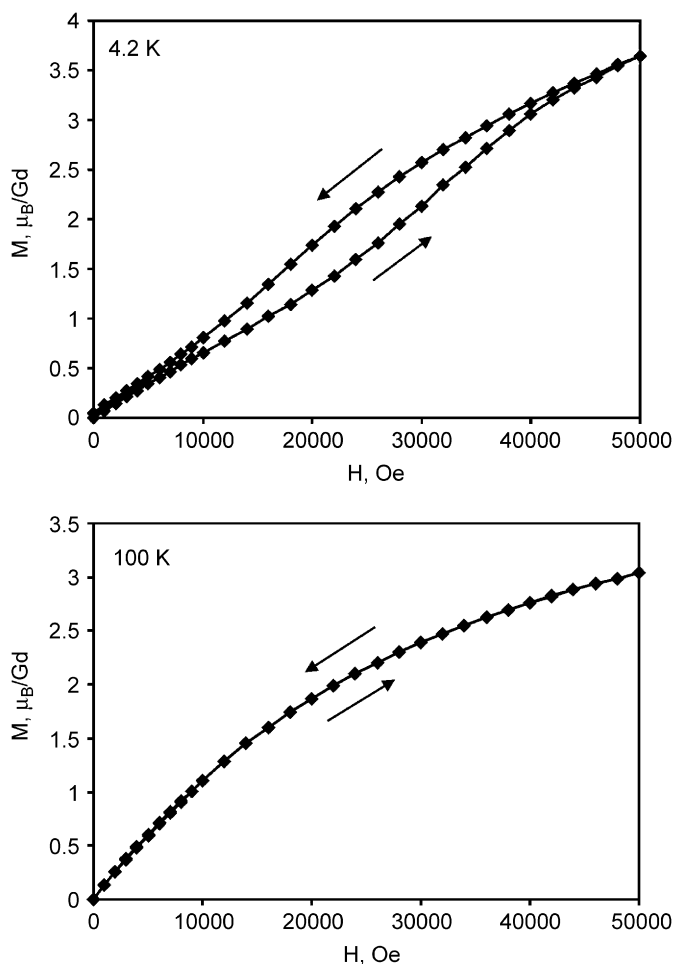


Fig. 2. Magnetization as a function of field for hexagonal  $Gd_5Bi_3$  at 4.2 and 100 K.

same could be assumed for  $Gd_5Sb_3$  and  $Gd_5Bi_3$ . Also based on the literature data for  $Gd_5Bi_3$  [5,6], it could be hypothesized that the same structural sequence is followed by  $Gd_5Bi_3$ , but this was never rigorously proven. To check for the existence of the HT  $Yb_5Sb_3$ -type polymorphs, the two binaries  $Gd_5Sb_3$  and  $Gd_5Bi_3$ , annealed at 800 °C, were sealed in tantalum tubes and annealed at 1350 °C in dynamic vacuum. After annealing at 1350 °C for 1.5 h,  $Gd_5Bi_3$  showed complete transformation from the  $Mn_5Si_3$ -type polymorph into the  $Yb_5Sb_3$ -type one. If  $Gd_5Bi_3$  treated at 1350 °C is annealed again at 800 °C for 2 weeks, it transforms back into the hexagonal polymorphs, proving that the  $Mn_5Si_3$ -type  $\leftrightarrow$   $Yb_5Sb_3$ -type transformation is fully reversible. On the other hand,  $Gd_5Sb_3$  showed no signs of structural rearrangements even after 6 h at 1350 °C, thus indicating that the orthorhombic structure is not accessible for  $Gd_5Sb_3$  at least at this temperature. Annealing of the  $Gd_5Sb_3$  and  $Gd_5Bi_3$  samples at 600 and 400 °C produced the same phases as annealing at 800 °C.

The " $A_5Pn_3$ " pnictides ( $A$  = a divalent electropositive atom such as Ca, Sr, Ba, Sm, Eu, Yb,  $Pn$  = Sb, Bi) with the  $Yb_5Sb_3$ -type structure have been shown to be, in reality, hydrogen-stabilized  $A_5Pn_3H$  phases, with hydrogen coming

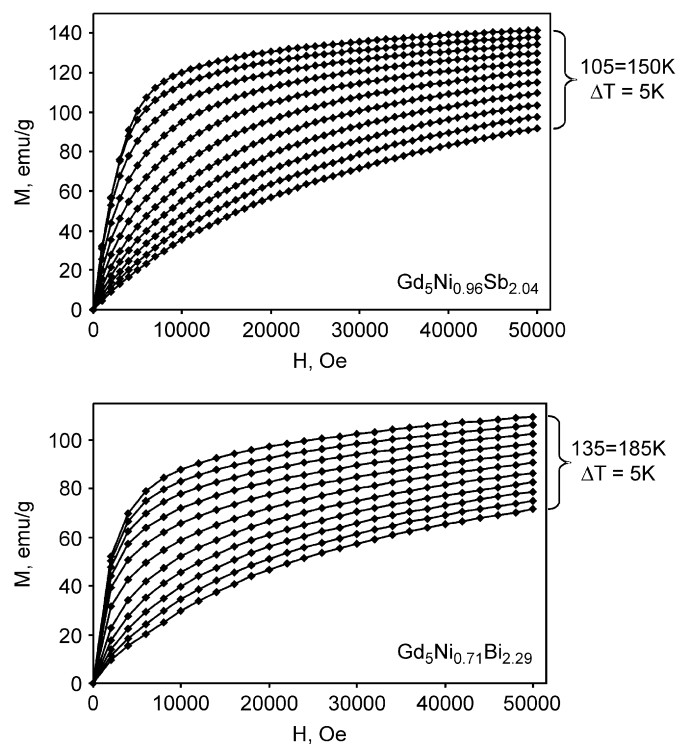


Fig. 3. Magnetization versus field curves for orthorhombic  $Gd_5Ni_{0.96}Sb_{2.04}$  and  $Gd_5Ni_{0.71}Bi_{2.29}$ .

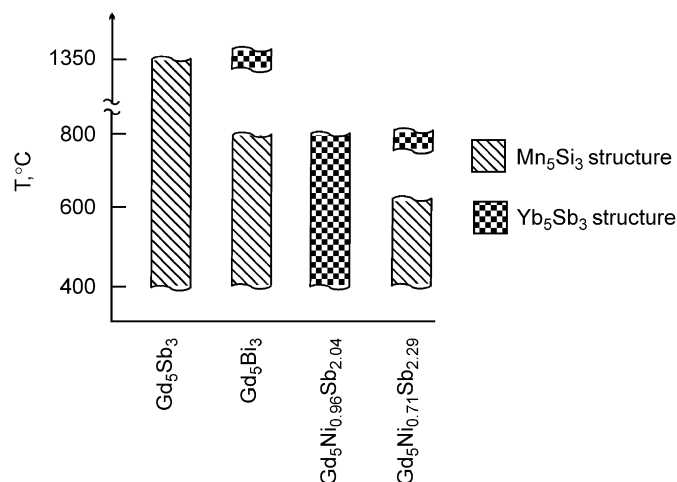


Fig. 4. Schematic phase diagram for  $Gd_5Sb_3$ ,  $Gd_5Bi_3$ ,  $Gd_5Ni_{0.96}Sb_{2.04}$  and  $Gd_5Ni_{0.71}Sb_{2.29}$ .

from the commercial  $A$  metals [11,12]. As Ta becomes relatively transparent to  $H_2$  above 550 °C, annealing under the dynamic vacuum at higher temperatures dehydrogenates the samples and results in the formation of the hexagonal  $A_5Pn_3$  phases (the  $Mn_5Si_3$ -type) [11]. While hydrogen presence is proven to be an important factor in the chemistry of pnictides with a divalent metal,  $A$ , its role in the stability of analogous pnictides with a trivalent rare-earth elements,  $RE$ , is not fully understood. Even if hydrogen tends to stabilize the  $RE_5Pn_3$  pnictides, the conditions of our experiment (1350 °C and dynamic

vacuum) are expected to dehydrogenate and, thus, preclude hydrogen stabilization of the high-temperature form of  $Gd_5Bi_3$  and also of the hexagonal  $Gd_5Sb_3$  phase.

The compositions  $Gd_5Ni_{0.96(1)}Sb_{2.04(1)}$  and  $Gd_5Ni_{0.71(1)}Bi_{2.29(1)}$  obtained from the single crystal refinements were Ni poorer than the initial ones used for the synthesis, therefore it was assumed that the Ni amounts in these phases were the largest ones accessible under our experimental conditions. Thermal stability of the  $Gd_5Ni_{0.96}Sb_{2.04}$  and  $Gd_5Ni_{0.71}Bi_{2.29}$  phases was studied through annealing at 600 °C for 1 week, followed by annealing at 400 °C for 2 weeks. At 600 and 400 °C,  $Gd_5Ni_{0.71}Bi_{2.29}$  was found to decompose into the hexagonal binary  $Gd_5Bi_3$  and an unidentified Ni-containing phase. The lattice constants of the obtained  $Gd_5Bi_3$  binary were in good agreement with those of the pristine  $Gd_5Bi_3$  sample, thus indicating that there was no nickel left in the resulting  $Gd_5Bi_3$  binary. We could not find suitable single crystals of hexagonal  $Gd_5Bi_3$  to confirm that no nickel is present. In contrast,  $Gd_5Ni_{0.96}Sb_{2.04}$  showed no signs of a structural transformation/decomposition at either 600 °C or 400 °C. While  $Gd_5Ni_{0.96}Sb_{2.04}$  may still undergo a phase transition at lower temperatures, this could require a very long annealing time as the atomic rearrangements associated with this transition are very significant (see the discussion below).

In addition to  $Gd_5Ni_{0.96}Sb_{2.04}$ , and  $Gd_5Ni_{0.71}Bi_{2.29}$  reported here, the orthorhombic  $Yb_5Sb_3$ -type structure is observed for other transition-metal substituted  $RE_5T_xSb_{3-x}$  and  $RE_5T_xBi_{3-x}$  phases annealed at 830 °C ( $RE$  is a rare earth and  $T = Fe-Cu$ ) [4,13]. Out of all possible  $RE_5T_xSb_{3-x}$  and  $RE_5T_xBi_{3-x}$  phases, only few representatives and only those without gadolinium were prepared. Besides, the thermal stability of these phases was not investigated. Based on our current studies and the literature data [4], it can be concluded that the substitution of a late 3d-metal for Sb or Bi tends to stabilize the orthorhombic polymorphs of the corresponding binaries at high temperatures (exception is  $Gd_5Ni_{0.96}Sb_{2.04}$ ). But this substitution by the transition metal is limited. The limited amount of Ni and the stability of the corresponding Ni-substituted orthorhombic phase were analyzed in details

for  $Y_5Ni_xSb_{3-x}$  [4]. It has been concluded that Ni incorporation reduces the strength of the Y–Sb interactions, which in turn limits the maximum amount of Ni in the structure. The structure can be stabilized only at high temperatures due to the entropy contribution stemming from the Ni/Sb statistical mixture. We can argue that the same is true for  $Gd_5Ni_{0.96}Sb_{2.04}$  and  $Gd_5Ni_{0.71}Bi_{2.29}$ .

The two structural polymorphs, the  $Mn_5Si_3$  and  $Yb_5Sb_3$  ones, differ significantly in terms of atomic arrangements (Fig. 5), and as pointed by Brunton and Steinfink [14] who first discovered the  $Yb_5Sb_3$  phase, there is little resemblance between the two structure types. In the “classical” presentation by Guloy et al. [15], the  $Mn_5Si_3$ -type structure of  $Gd_5Bi_3$  is constructed from the Gd1 octahedra that are fused along the  $c$  direction to form hexagonal columns. The columns are interconnected through the Bi atoms, which in turn form channels filled with Gd2 chains. While hexagonal channels can be also identified in the  $Yb_5Sb_3$ -type structure of  $Gd_5Bi_3$ , they are irregular and filled with both Gd and Bi atoms (Fig. 5). There are also the trigonal channels filled with the Bi atoms and attached to the hexagonal ones. No simple atomic rearrangement is found to transform one structure into the other, besides the space groups of the two structures are not in a group–subgroup relationship. Such different atomic arrangements may explain the fact that the HT orthorhombic polymorphs could be easily quenched into room temperature and that a long annealing time is required to obtain a LT hexagonal polymorph.

### 3.2. Magnetic properties and magnetocaloric effect

The LT hexagonal polymorph of  $Gd_5Bi_3$  exhibits a complex magnetic behavior (Fig. 1) which is analogous to that found in hexagonal  $Gd_5Sb_3$  [8]. While the overall shape of the curve may be representative of an antiferromagnetic ordering, the Weiss temperature derived from the paramagnetic region clearly indicates that interactions at higher temperatures are ferromagnetic in nature. These ferromagnetic interactions yield a ferromagnetic ordering at 112 K, followed by a significant decrease in magnetization below 64 K which is indicative of spin reorientation. A

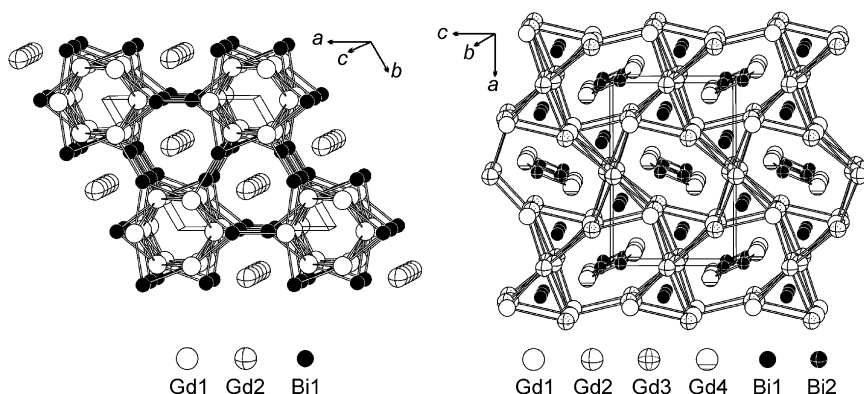


Fig. 5. Structures of the hexagonal  $Mn_5Si_3$ -type (left) and orthorhombic  $Yb_5Sb_3$ -type (right) polymorphs of  $Gd_5Bi_3$ .

step-like change in  $M$  vs.  $H$  at 4.2 K also points at spin reorientation at low temperatures (Fig. 2). This step-like feature is expected to be absent above 64 K, and this is verified by a  $M$  vs.  $H$  scan at 100 K. At both temperatures 4.2 and 100 K, magnetization in 50 kOe did not reach the  $gJ$  value of  $7.00 \mu_B$  expected for a  $Gd^{3+}$  free ion. Above 200 K,  $Gd_5Bi_3$  follows the Curie–Weiss law with  $\theta_p = 137$  K and  $\mu_{\text{eff}/Gd} = 8.57 \mu_B$  (Table 4). For comparison, at the paramagnetic region the HT orthorhombic form of  $Gd_5Bi_3$  obeys the Curie–Weiss law with  $\theta_p = 120$  K and  $\mu_{\text{eff}/Gd} = 8.43 \mu_B$  [6], while hexagonal  $Gd_5Sb_3$  follows the Curie–Weiss law with much larger  $\theta_p = 267$  K and  $\mu_{\text{eff}/Gd} = 10.9 \mu_B$  [8].

The orthorhombic  $Gd_5Ni_{0.96}Sb_{2.04}$  and  $Gd_5Ni_{0.71}Bi_{2.29}$  compounds undergo ferromagnetic orderings at 115 and 162 K, respectively. Interestingly, the Curie temperature for the Ni-substituted  $Gd_5Ni_{0.71}Bi_{2.29}$  is 50 K higher than that of the pure orthorhombic  $Gd_5Bi_3$  binary. At higher temperatures, both Ni-substituted phases obey the Curie–Weiss relationship with  $\theta_p = 161$  K and  $\mu_{\text{eff}/Gd} = 8.48 \mu_B$  for  $Gd_5Ni_{0.96}Sb_{2.04}$  and  $\theta_p = 182$  K and  $\mu_{\text{eff}/Gd} = 9.61 \mu_B$  for  $Gd_5Ni_{0.71}Bi_{2.29}$ . The calculated magnetic moment for Gd in  $Gd_5Ni_{0.96}Sb_{2.04}$  is similar to those observed in orthorhombic and hexagonal  $Gd_5Bi_3$ , thus suggesting that magnetic contribution of Ni atoms is small. Even if assumed otherwise, the Ni contribution would be insufficient to yield large magnetic moments observed in  $Gd_5Ni_{0.96}Sb_{2.04}$  and especially in  $Gd_5Ni_{0.71}Bi_{2.29}$ . It is also difficult to say whether the Ni presence influences the Gd moment since the phases with the same structure have to be compared. However only two Gd-containing phases,  $Gd_5Bi_3$  and  $Gd_5Ni_{0.71}Bi_{2.29}$ , with the same  $Yb_5Sb_3$ -type structure are known, and thus no general conclusions can be drawn.

Magnetic moments larger than  $\mu_{\text{eff}} = g[J(J+1)]^{1/2} \mu_B = 7.94 \mu_B$  expected for a free  $Gd^{3+}$  ion are found not only in  $Gd_5Bi_3$ ,  $Gd_5Sb_3$  and their Ni derivatives, but also in other Gd-containing phases: e.g.  $8.32 \mu_B$  in  $Gd_4Pd_{10}In_{21}$  [16]. Even elemental Gd shows a  $\sim 9\%$  increase for its measured magnetic moment [17]. Generally, increase in  $\mu_{\text{eff}/Gd}$  is attributed to the polarization of conduction electrons, predominantly the Gd  $5d$  ones, through the  $4f$ – $5d$  exchange interactions [18,19].

Magnetocaloric effect in terms of entropy change,  $\Delta S$ , for the Ni-substituted materials was evaluated from the magnetization data (Fig. 3) using the Maxwell relation-

ships [3]:

$$\left(\frac{\partial S(T, H)}{\partial H}\right)_T = \left(\frac{\partial M(T, H)}{\partial T}\right)_H,$$

which after the integration yields  $\Delta S(T)_{\Delta H} = \int_{H_1}^{H_2} (\partial M(T, H)/\partial T)_{H,P} dH$ . In practice, a numerical integration is performed using the following formula:

$$\Delta S(T)_{\Delta H} = \sum_i \frac{M_i - M_{i+1}}{T_{i+1} - T_i} \delta H,$$

where  $\delta H$  is a magnetic field step and  $M_i$  and  $M_{i+1}$  are the

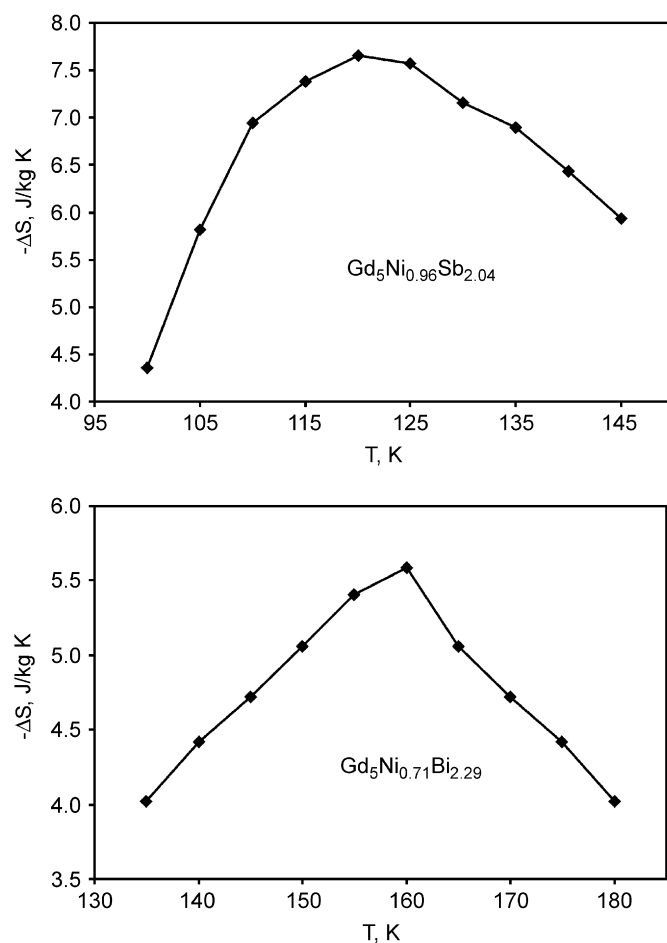


Fig. 6. Entropy change for  $Gd_5Ni_{0.96}Sb_{2.04}$  and  $Gd_5Ni_{0.71}Bi_{2.29}$  as a function of temperature for  $\Delta H = 0$ – $50,000$  Oe.

Table 4  
Magnetic parameters for  $Gd_5Sb_3$ ,  $Gd_5Bi_3$ ,  $Gd_5Ni_{0.96}Sb_{2.04}$  and  $Gd_5Ni_{0.71}Bi_{2.29}$

Compound	Space group	Magnetic behavior	$T_C$ (K)	$\mu_{\text{eff}/Gd}$ , ( $\mu_B$ )	$\theta_p$ (K)	$-\Delta S$ (J/kg K)	Ref.
$Gd_5Sb_3$	$P6_3/mcm$	Ferromagnetic	187	10.9	266.8		[8]
$Gd_5Ni_{0.96}Sb_{2.04}$	$Pnma$	Ferromagnetic	115	8.48	161	7.7 <sup>a</sup>	This work
$Gd_5Bi_3$	$P6_3/mcm$	Ferromagnetic	112	8.57	137		This work
$Gd_5Bi_3$	$Pnma$	Ferromagnetic	110	8.43	120		[6]
$Gd_5Ni_{0.71}Bi_{2.29}$	$Pnma$	Ferromagnetic	162	9.61	182	5.6 <sup>a</sup>	This work

<sup>a</sup>  $\Delta S$  is the maximum entropy change for a magnetic field change  $\Delta H = 0$ – $50,000$  Oe.

values of magnetization at temperatures  $T_i$  and  $T_{i+1}$ , respectively. The magnetic entropy change,  $\Delta S$ , for  $\Delta H = 0\text{--}50,000$  Oe is plotted in Fig. 6. As expected,  $\Delta S$  peaks around the Curie temperatures and has the maximum value of  $-7.7$  J/kg K for  $\text{Gd}_5\text{Ni}_{0.96}\text{Sb}_{2.04}$  and  $-5.6$  J/kg K for  $\text{Gd}_5\text{Ni}_{0.71}\text{Bi}_{2.29}$ . While these values of  $\Delta S$  are substantial, they are smaller (by absolute values) than  $-9.8$  J/kg K measured for pure gadolinium or  $-18.5$  J/kg K found for  $\text{Gd}_5\text{Si}_2\text{Ge}_2$  [1].

#### 4. Conclusion

The two binaries  $\text{Gd}_5\text{Sb}_3$  and  $\text{Gd}_5\text{Bi}_3$  exhibit different structural behavior with temperature.  $\text{Gd}_5\text{Bi}_3$  adopts two polymorphs: a LT  $\text{Mn}_5\text{Si}_3$ -type one below  $800^\circ\text{C}$  and a HT orthorhombic  $\text{Yb}_5\text{Sb}_3$ -type one at  $1350^\circ\text{C}$ . In contrast,  $\text{Gd}_5\text{Sb}_3$  crystallizes only with a hexagonal  $\text{Mn}_5\text{Si}_3$ -type structure and is not found to undergo any structural transition up to  $1350^\circ\text{C}$ . Ni substitution leads to the formation of the orthorhombic structure for  $\text{Gd}_5\text{Ni}_{0.96}\text{Sb}_{2.04}$  and stabilizes the orthorhombic bismuthide  $\text{Gd}_5\text{Ni}_{0.71}\text{Bi}_{2.29}$  to lower temperatures.

The magnetic behavior of orthorhombic  $\text{Gd}_5\text{Ni}_{0.96}\text{Sb}_{2.04}$  and  $\text{Gd}_5\text{Ni}_{0.71}\text{Bi}_{2.29}$  is similar as both phases order ferromagnetically at low temperatures. Hexagonal  $\text{Gd}_5\text{Bi}_3$  shows a more complex magnetic behavior as the ferromagnetic ordering is followed by spin reorientation.

#### Acknowledgments

This work was supported by a Discovery Grant from the Natural Sciences and Engineering Research Council of Canada.

#### References

- [1] V.K. Pecharsky, K.A. Gschneidner Jr., Phys. Rev. Lett. 78 (1997) 4494–4497.
- [2] V.K. Pecharsky, K.A. Gschneidner Jr., Springer Series in Materials Science 79 (2005) 199–222 (Magnetism and Structure in Functional Materials).
- [3] A.M. Tishin, Y.I. Spichkin, The Magnetocaloric Effect and its Application, Institute of Physics Publishing, Bristol and Philadelphia, 2003.
- [4] Y. Mozharivskiy, H.F. Franzen, J. Alloys Compd. 319 (2001) 100–107.
- [5] K. Yoshihara, J.B. Taylor, L.D. Calvert, J.G. Despault, J. Less-Common Metals 41 (1975) 329–337.
- [6] J. Szade, M. Drzyzga, J. Alloys Compd. 299 (2000) 72–78.
- [7] W. Rieger, E. Parthe, Acta Crystallogr. B 24 (1968) 456–458.
- [8] M. Nagai, A. Tanaka, Y. Haga, T. Tsubotaoka, J. Magn. Mater. 310 (2007) 1775–1777.
- [9] B.A. Hunter, C.J. Howard, Rietica, Australian Nuclear Science and Technology Organization, Menai, Australia, 2000.
- [10] G.M. Sheldrick, SHELXL97 and SHELXS97, University of Göttingen, Germany, 1997.
- [11] E.A. Leon-Escamilla, J.D. Corbett, J. Alloys Compd. 265 (1998) 104–114.
- [12] E.A. Leon-Escamilla, J.D. Corbett, Chem. Mater. 18 (2006) 4782–4792.
- [13] A.V. Morozkin, R. Nirmala, S.K. Malik, J. Alloys Compd. 394 (2005) L9–L11.
- [14] G.D. Brunton, H. Steinfink, Inorg. Chem. 10 (1971) 2301–2303.
- [15] A.M. Guloy, A.-V. Mudring, J.D. Corbett, Inorg. Chem. 42 (2003) 6673–6681.
- [16] Y. Verbovytsky, K. Latka, A.W. Pacyna, J. Alloys Compd. 442 (2007) 337–340.
- [17] L.W. Roeland, G.J. Cock, F.A. Muller, A.C. Moleman, K.A. McEwen, R.G. Jordan, D.W. Jones, J. of Phys. F: Metal Phys. 5 (1975) L233–L237.
- [18] B.N. Harmon, A.J. Freeman, Phys. Rev. B: Solid State 10 (1974) 1979–1993.
- [19] G. Czjzek, V. Oestreich, H. Schmidt, K. Latka, K. Tomala, J. Magn. Mater. 79 (1989) 42–56.